The Aeronautical Journal (2024), 1–15
doi:10.1017/aer.2024.41

REGULAR PAPER

Experimental analysis of noise disturbances generated by reaction wheel

A. Mankour, A. Smahat, E.H. Bensikaddour and R. Roubache

Department of Research in Space Mechanics, Satellite Development Center (CDS), BP4065, Ibn Roched, Oran 31100, Algeria
Corresponding author: A. Mankour; Email: ajmankour@cds.asal.dz

Received: 6 November 2023; **Revised:** 3 March 2024; **Accepted:** 28 March 2024

Keywords: reaction wheel test; disturbance noise; imbalance; rotation speed; imperfection

Abstract

Microvibrations originating from onboard disturbance sources can lead to a range of issues, including a decrease in satellite pointing accuracy, image distortion and blurring. Therefore, reaction wheels emerge as the primary sources of disturbance noise. This paper employs an experimental approach based on the real dynamics of rotating reaction wheel assembly, closely simulating on-orbit configurations to measure noise responses transferred to the satellite structure. An assessment of noise response behaviour, incorporating a comprehensive understanding of the factors influencing the levels, was conducted on a proto-flight satellite for three reaction wheels. Initially, reaction wheel assemblies underwent individual iterative balancing to reduce mass deviations. Subsequently, amplitude-time responses at different rotational speeds of reaction wheel assemblies (RWA) disturbance noise were measured. The experimental results demonstrate that each individually balanced reaction wheel generates independent perturbation noise level due to manufacturing imperfections. Hence, the necessity of wheels testing for accurate prediction and mitigation of disturbance levels is crucial, especially for payloads sensitive to microvibrations. Furthermore, increasing wheel speeds proportionally amplify disturbance noise levels. Therefore, implementing an optimised mission attitude control profile with lower rotation speeds of reaction wheels effectively reduces microvibration levels which minimises risks to payload performance and reduce power consumption.

Nomenclature

ST	Satellite Technologies
RWA	Reaction Wheel Assembly
MAI	Maryland Aerospace Incorporated
SSTL	Surrey Satellite Technology Limited
RW	Reaction Wheel
Δms	unbalance mass
Us	Static Unbalance
R	radius
ω	Angular velocity
CG	Center of Gravity
Ts	Static Disturbance
ud	dynamic Unbalance
RPM	Revolutions Per Minute
SF	Safety Factor
PFM	Proto-Flight Model
ACS	Attitude Control Systems

1.0 Introduction

As satellite technologies continue to advance, and the demand for systems that offer high resolution, exceptional agility and cost-effectiveness intensifies, there is a noticeable trend toward the integrated design of satellite platforms and their corresponding payloads. This tendency is particularly gaining importance concerning earth observation satellites and space telescopes due to the continuous evolution of optical payloads, which are becoming increasingly advanced and sensitive. Reaction wheels (RWs) are common actuators in the attitude control system of satellites, generating the desired torque for stability and orientation requirements. High control precision of reaction wheels is therefore a key device to meet the required pointing accuracy of the satellite. However, the rotation of the reaction wheel induces torque and force disturbances which degrade the satellite attitude stability quality. Hence, the vibrational loads and torque disturbances are inherent in this type of rotating actuator. Reaction wheels are the main disturbance source onboard the satellite as they create microvibrations [1–3].

The choice of reaction wheels for a microsatellite is determined by mission requirements, including size, weight, power constraints and performance specifications. Several off-the-shelf suppliers offer a variety of options, such as Goodrich Corporation (types AA, A, B, C and E), Honeywell International (HR0610), L-3 Communications (RWA-15, MWA-50), Maryland Aerospace, Inc. (MAI-101 and MAI-201), Bradford Engineering (W05, W18, and W45), Microsat Systems Canada Inc. (MicroWheel 200, 1,000, and 4,000), Rockwell Collins (TELDIX RWs) and Surrey Satellite Technology Ltd. (10SP-M, 100SP-M, and 200SP) [4]. RW's disturbances can originate from various wheel-internal sources, such as inertia wheel imbalance, bearing torque noise due to imperfections, bearing friction effects, motor torque ripple and motor cogging [5]. Due to anomalies potential issues, the use of each RW's model require that every single wheel undergoes meticulous balancing and individual noise disturbance testing. Consequently, the level of disturbance noise of the same wheel class should be measured by test.

Micro-vibrations occurring within spacecraft represent a distinct form of vibration characterised by their small amplitude and high frequency, typically exerting negligible influence on the structural integrity. Nevertheless, these micro-vibrations, stemming from various sources, traverse the satellite's structure, provoking resonant modes in both the structure and instrument components, thereby affecting their performance [6, 7]. Microvibrations are usually within the g scale but their frequency content may vary from 1 Hz to 2 kHz [5]. Nonetheless, when it comes to sub-meter satellites, micro-vibrations have emerged as an essential factor significantly impacting the quality of high-resolution images [8].

The disturbances are mainly due to static and dynamic imbalances of the wheel which affect pointing accuracy and consequently the imaging quality [9–11]. There are two types of imbalances that are usually distinguished. The first is the static imbalance, which appears when the RW centre of mass is not located at its rotation axis. The second is the dynamic imbalance, which corresponds to the misalignment between the RW principal axis of inertia and the rotation axis [12]. The dynamic imbalance induces the torque directly on the satellite body. These disturbances affect the attitude stability quality of the spacecraft, and cannot ensure the required precision pointing [13, 14].

Reaction wheels are the dominant source of high-amplitude jitter disturbance in several satellite missions due to static and dynamic imbalances within reaction wheel assemblies. Each imbalance can be modeled as shown in Fig. 1 [15, 16]. Static imbalance is the condition where the principal inertia axis of a rotor is offset from and parallel to the axis of rotation.

Static imbalance can theoretically be adjusted by adding a single correction mass. Thus, the disturbance caused by the static imbalance can be expressed as follows:

$$\begin{aligned} F_s &= M_r\omega^2 \\ &= \Delta m_s r\omega^2 \\ &= u_s\omega^2 \end{aligned} \tag{1}$$

where: Δm_s is the unbalance mass that causes static imbalance, u_s is the static imbalance, r is the radius of the wheel and ω is the angular velocity of the wheel.

https://doi.org/10.1017/aer.2024.41 Published online by Cambridge University Press

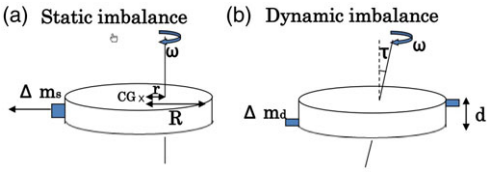

Figure 1. *Disturbance model of (a) static imbalance and (b) dynamic imbalance.*

If the reaction wheel is mounted at a distance "l" from the centre of gravity (CG), then the disturbance torque caused by the static imbalance is:

$$T_s = u_s \omega^2 l \tag{2}$$

where: T_s is the static disturbance torque, l is the distance from the wheel CG.

Dynamic imbalance is the condition where the principal inertia axis is not parallel to rotation axis, as shown in Fig. 1. The disturbance torque caused by the dynamic imbalance is quantified as follows:

$$\begin{aligned} T_d &= \Delta m_d r d \omega^2 \\ &= u_d \omega^2 \end{aligned} \tag{3}$$

where: T_d is the dynamic disturbance torque, u_d is dynamic imbalance and d is the axial length between the imbalance masses.

Note that the rotor imbalance induces a centripetal force at the frequency of the rotation.

For these reasons, reducing the imbalances of the rotating flywheel is necessary during the wheel manufacturing stage [17, 18]. Hence, the influence of disturbances on the quality of the attitude control should be analysed prior to the application of the wheels on the satellite [19]. In addition, predicting wheel disturbances due the manufacturing imperfection remains an open challenge [20].

The accurate measurement of disturbance generated by reaction wheels and understanding the factors influencing their magnitude are crucial for various aspects of satellite design. These include monitoring the health of reaction wheels, designing attitude control systems, enhancing payload performance and validating satellite finite element models. The test results can inform the development of strategies for microvibration isolation or suppression by adjusting the transmission path through the structural design of the spacecraft or payload [21, 22], thus facilitating the design of effective isolation systems to mitigate microvibration impact. Additionally, these results contribute to optimising the rotational speed of RWs used in designing attitude control profiles [23].

There are a number of approaches used to reduce RW vibrations' influence. In the study of Ref. [23], small and low-speed RWs are used to reduce the effect of jitter and power consumption. In the study of Ref. [24], a special platform is proposed and studied. A similar platform and mass dampers are described by the authors of Ref. [25, 26] to achieves low-frequency motion transmission and high-frequency vibration isolation. In the study of Ref. [27], a two-stage scheme is proposed for the satellite with precise optical payload. In general, different vibration isolation techniques are presented in the survey in Ref. [28]. The RW construction improvement is also considered. Hence, the results of liquid RWs in flight operation are presented in the study of Ref. [29], and they show low vibration level. Enhancing the design of the disturbance source to refine machining accuracy or altering the spacecraft's structural design to modify the transmission path of micro-vibrations involves higher costs and longer qualification processes. Although, implementing vibration isolation devices offers an efficient strategy for micro-vibration suppression without requiring major spacecraft design changes. Placing these devices strategically, between the spacecraft bus and the disturbance source to curtail micro-vibration propagation to the spacecraft platform [30], or between the spacecraft and sensitive payloads to attenuate micro-vibration transmission [31], has been recognised as a highly effective approach [29, 32].

https://doi.org/10.1017/aer.2024.41 Published online by Cambridge University Press

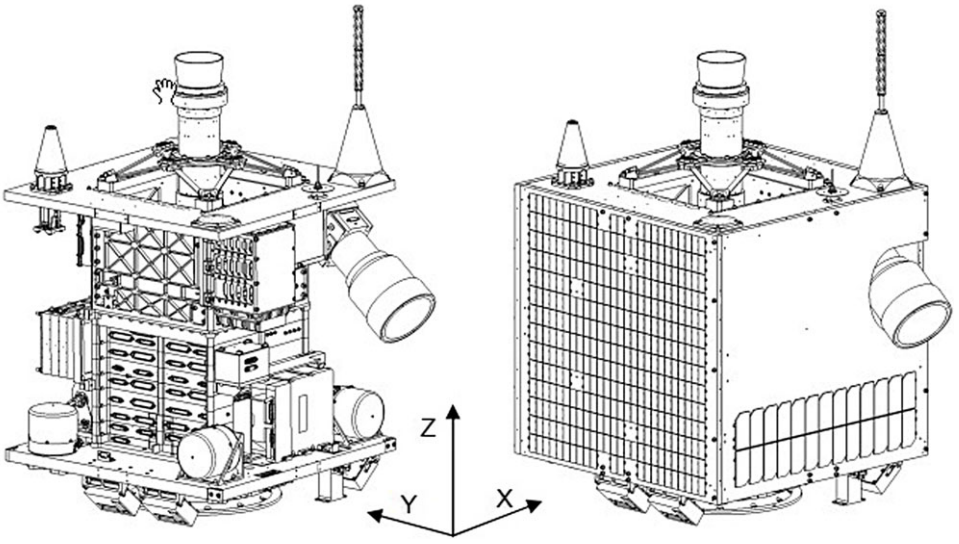

Figure 2. *ALSAT 1B observation satellite.*

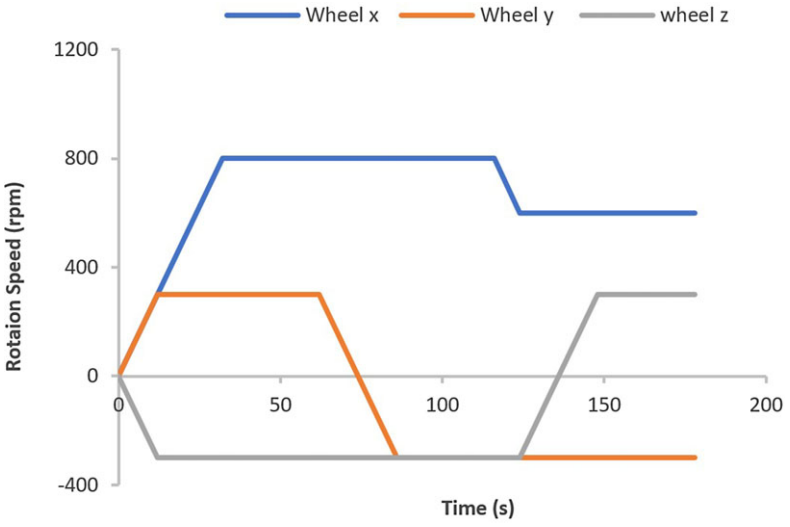

Figure 3. *Alsat-1B wheel rotational speed profile.*

This paper presents an experimental investigation into the disturbance noise behaviour originating from rotating reaction wheels closely replicating on-orbit configuration within the proto-flight model of the ALSAT 1B observation satellite (Fig. 2). The study aims to accurately measure disturbance levels transferred to the satellite structure, with a specific focus on assessing the impact of manufacturing imperfections and trends in rotational speed variation on its magnitude. To ensure compliance with balance requirements, static and dynamic balancing procedures were conducted on the three reaction wheels prior to conducting the disturbance noise test. Subsequently, each reaction wheel assembly (RWA) mounted on the spacecraft underwent individual tests to measure the disturbance level generated and transferred to the satellite structure. The analysis focuses on key factors, including the influence of manufacturing imperfections on disturbance levels and noise trend according to rotational speed variations. Note that the worst-case scenario of wheel rotation allocated for satellite stabilisation during imaging is highlighted in Fig. 3.

https://doi.org/10.1017/aer.2024.41 Published online by Cambridge University Press

Table 1. *Reaction wheel characteristics [33].*

Wheel type	Peak Momentum	Peak Torque	Mass	Power Constant Speed
10SP-M	0.42 Nms	11 mNm	0.99 kg	0.7 W

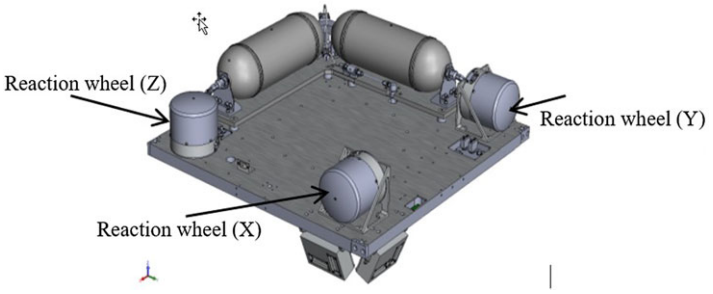

Figure 4. *Reaction wheels configuration.*

2.0 Materials and method

The experimental test of noise disturbance was achieved using the proto-flight model of Alsat 1B (Fig. 2) which uses three RWA's for the pointing accuracy and stabilisation toward the three axes (X, Y and Z). Hence, the configuration of the three wheels on the satellite is shown in Fig. 4. In addition, the characteristics of reaction wheels (10SP-M) are also reported in Table 1.

2.1 Experimental description and setup

For noise test, we need to balance the three wheels statically and dynamically separately. Thus, each test belongs a test procedure as follows:

2.1.1 Static and dynamics balancing

- Balancing mechanical setup:

To achieve the balancing of wheels shows a basic setup with the 10SP-M wheel illustrated in the Fig. 5. The interface plate is bolted to the balancing sense pillars, which are in turn bolted to the test bed. The wheel is bolted to their interface plates and sense pillars are fitted.

- Balancing test procedure:

Once testing begins, the wheel is commanded via the computer to achieve a constant speed 2000 RPM for 10 SP-M wheels (Fig. 6). The faster the wheel rotates, the greater the resolution of the unbalance measurements. The balancing machine then calculates the mass and position (in terms of hole numbers) required for balancing. The wheel is then commanded to stop, grub screws are then inserted into the specified hole and the measurement is repeated. The objective was to bring the mass required to balance the wheel within the tolerances.

- Balance requirements:

Table 2 gives the typical static and dynamic balance requirements for microsatellite wheels.

https://doi.org/10.1017/aer.2024.41 Published online by Cambridge University Press

Table 2. *Static and dynamic balance requirements for 10SP wheels*

Balance Requirement	Value
Static unbalance	<0.1 g.cm
Dynamic unbalance	<0.2 g.cm^2

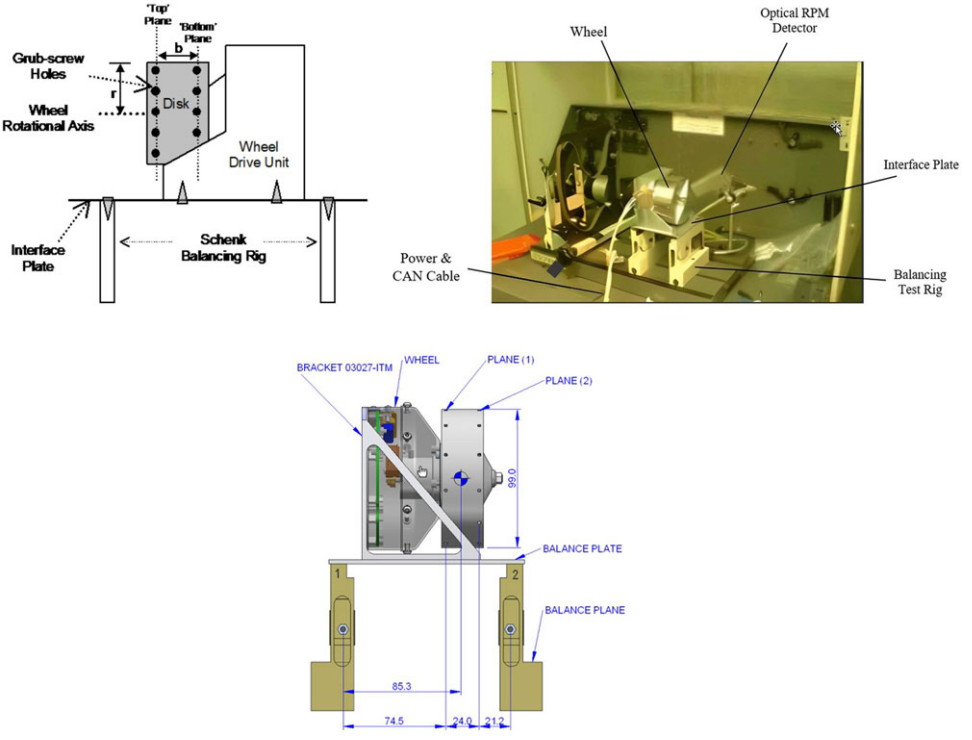

Figure 5. *Balancing setup (rig & wheel).*

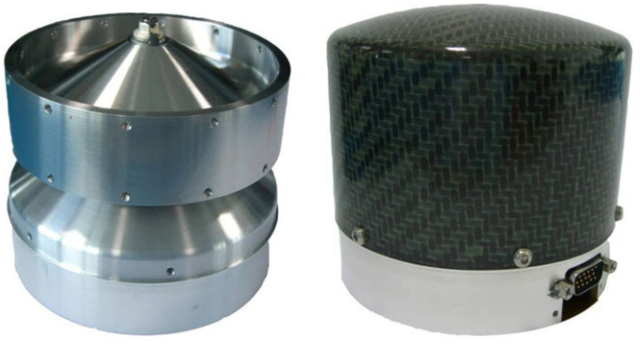

Figure 6. *Single reaction wheel 10SP-M [34, 35] (without and with cover).*

https://doi.org/10.1017/aer.2024.41 Published online by Cambridge University Press

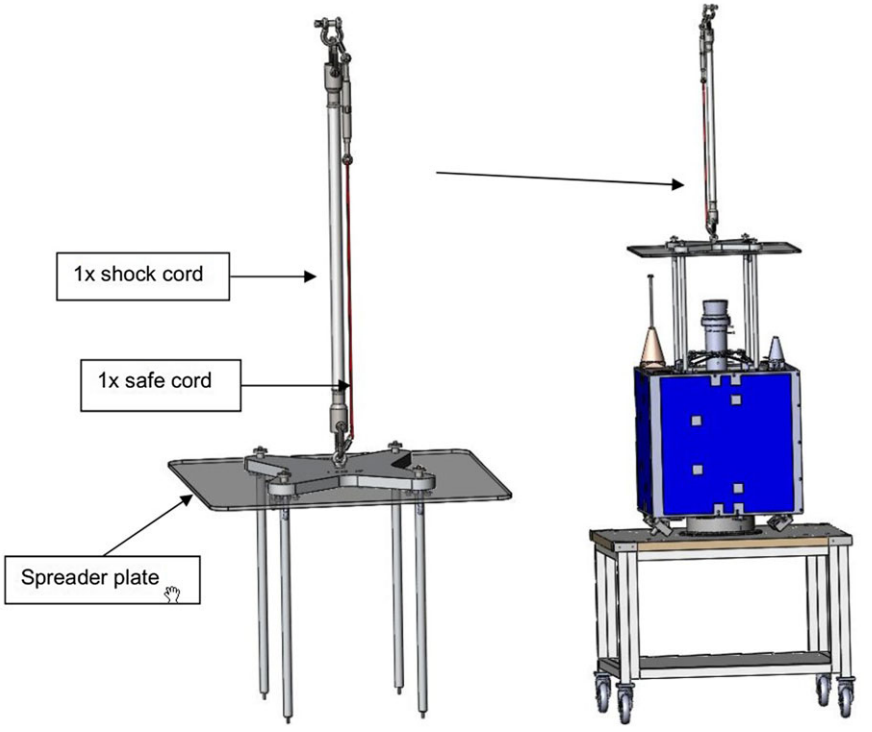

Figure 7. *Scheme of spacecraft configuration for disturbance noise test.*

2.1.2 Wheel noise quantification

Tests were conducted on the proto-flight model (PFM) spacecraft to evaluate the disturbance noise generated by the reaction wheels used on the Alsat-1b platform. Given the need for an environment with extremely low levels of microvibrations, the testing was performed in a highly quiet setting, with the wheel disturbance assessments taking place during nighttime. Furthermore, to minimise the ambient noise in the testing environment, the air conditioning in the clean room was turned off.

Throughout the testing process, the spacecraft was suspended vertically and supported by a shock cord, as depicted in Fig. 7. This shock cord served two primary purposes during the testing. Firstly, it effectively protected the satellite from any external vibrations that could have originated from the construction's floor. Secondly, it allowed the boundary conditions of the test item to closely resemble those experienced in orbit, thus enhancing the accuracy of the testing process. Moreover, safety cord is additional precautionary measures used as redundancy to secure the satellite in case of unexpected incident. The noise level measurement was conducted using a rotating wheel ranging from 0 to 1,000 RPM, with increments of 100 RPM.

Note that these tests do not entirely replicate the conditions encountered in orbit. The absence of factors such as the weight of the wheels and the spacecraft, along with the damping effects from the surrounding air, leads to a simulation that may not fully capture the dynamic behaviour experienced in space. Consequently, the results are adjusted by a safety factor (SF), which accounts for the differences observed between ground-based testing and actual in-orbit conditions, as identified in previous missions.

- Accelerometers positions:

To quantify the level of disturbance noise generated by RWs, we installed five (05) piezoelectric accelerometers (PCB 333B50) on the supporting plate positioned at the midpoint of the reaction wheel

https://doi.org/10.1017/aer.2024.41 Published online by Cambridge University Press

Table 3. *Accelerometers positions*

Channel N°	Description	Assigned reference
1	Cola Signal	101
2	Y Wheel	22X
3	Y Wheel	22Y
4	Y Wheel	22Z
5	Z Wheel	23Z
6	X Wheel	24Z

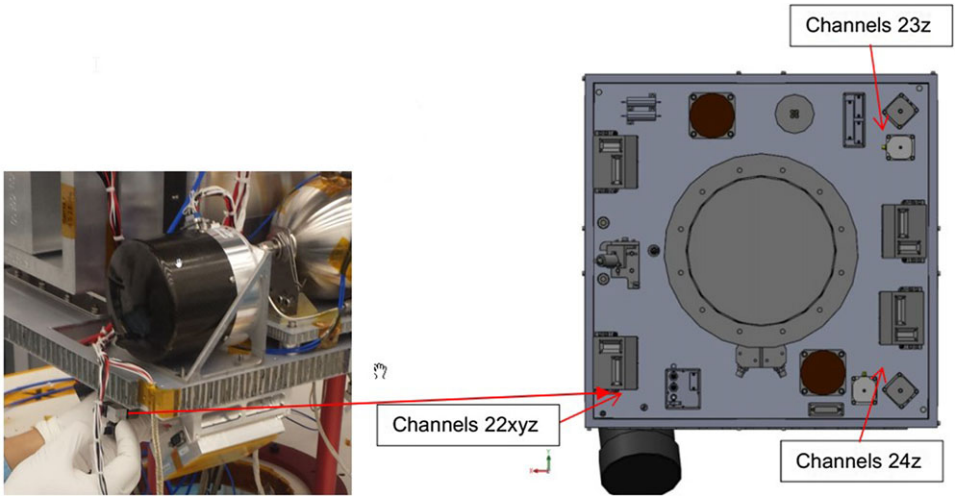

Figure 8. *Accelerometer positions for noise response.*

bolt pattern, as illustrated in Fig. 8. Additionally, we deployed an extra accelerometer (101) to monitor ambient noise perturbation that could potentially influence the measurement results.

The table below provides information on the data acquisition channel numbers and their corresponding locations on the spacecraft utilised during the noise disturbance tests (Table 3).

3.0 Results and discussions

3.1 Static and dynamic imbalance

The imbalance test correction was carried out on the three wheels separately. Thus, a mass balancing system was utilised to reduce the gap between the centre of mass and centre of rotation, thereby mitigating gravity disturbance.

As the grub screw positions are discrete and there is a limit to the balance mass that can be fitted at each location, there were cases when the mass indicated are greater than the limit. In this instance the mass should be distributed between adjacent locations of the same correction plane. The total balance mass for the plane is the vector product of the added masses at each location.

We note that, the required balance masses will become smaller and smaller for each iteration. Generally, initial balancing can be achieved using the variation in grub sizes. We note that, the balance has an acceptance band, the residual unbalance does not have to be zero. Therefore, the masses and location reported by the balance machine can be altered to purposely offset the balance to enable larger masses to be used.

https://doi.org/10.1017/aer.2024.41 Published online by Cambridge University Press

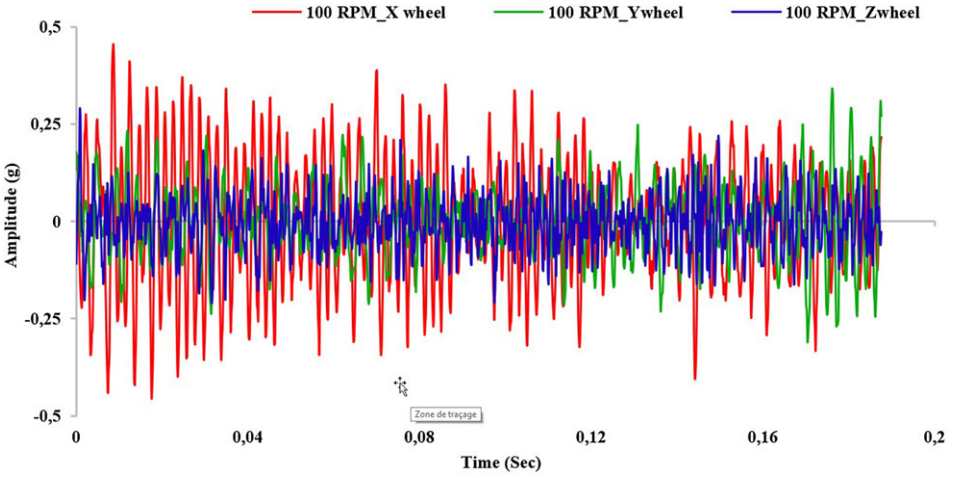

Figure 9. *Disturbance noise level vs. time for X, Y and Z wheels at 100 RPM.*

The balancing results are presented as follows:

- For static unbalance (g.cm): 0.059871
- For dynamic unbalance (g.cm^2): 0.037485

The outcome of the test indicated that the wheels satisfied the static unbalance requirement of < 0.1 g.cm^2 and the dynamic unbalance requirement of < 0.2 g.cm^2. As such, calibration was performed on each wheel individually to address the centre of mass shift resulting from manufacturing imperfections. Moreover, correction of the imbalance through this process enabled the effective reduction of the disturbance forces caused by both static and dynamic imbalance [36, 37].

3.2 Disturbance noise assessment

Extensive experimental evaluations were conducted to measure and mitigate the internal disturbances of the reaction wheels.

3.2.1 Wheels manufacturing imperfection assessment

An experiment was carried out to quantify the disturbance noise produced by the three wheels that were utilised to stabilise the proto-flight satellite. The outcomes were extracted and compared for the same rotational speed of the three RWAs. Figures 9–12 depict the experimental results obtained for the disturbance level of the three wheels at different rotational speeds (100, 300, 600, 1,000 RPM). Furthermore, the perturbation noise generated was extracted from a 0.2 second test.

We note that the three wheels were balanced statically and dynamically before noise disturbance test; hence, the noise disturbance still existing due to rotor unbalances and ball bearing vibration which amplify wheel resonances [38]. The experimental data indicates that, a considerable difference of generated disturbance noise in terms of magnitude from reaction wheel to another, which belong to the same manufacturing class. Even though the wheels are very accurately balanced statically and dynamically causes dynamic disturbances to the spacecraft with variation in bearing disturbance amplitudes [20]. Hence, imperfections due to manufacturing process in the same source equipment can lead to dissimilar behaviour of the wheel basing on generated vibration response [39, 40]. In addition, the interaction between vibrations engendered by defects in reaction wheels and spacecraft elements can be significant [41, 42]. Thus, examining the disturbance properties of RWs, which serve as a critical component in a

https://doi.org/10.1017/aer.2024.41 Published online by Cambridge University Press

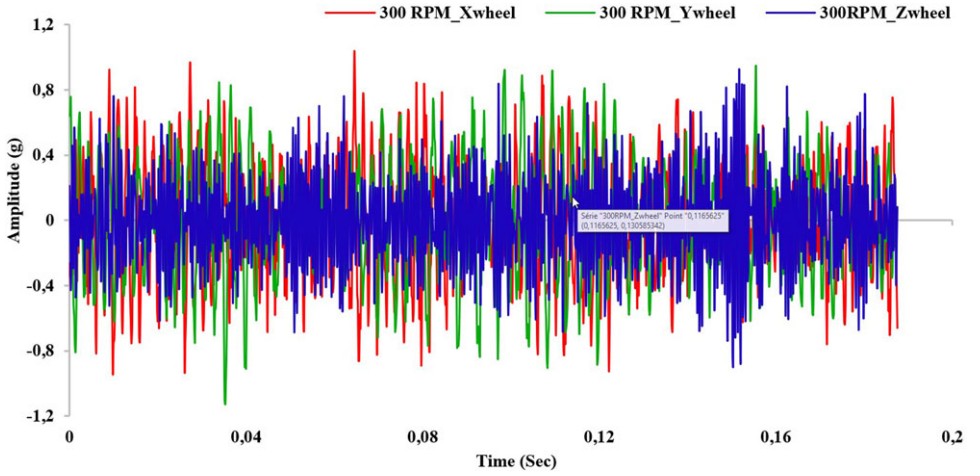

Figure 10. *Disturbance noise level vs. time for X, Y and Z wheels at 300 RPM.*

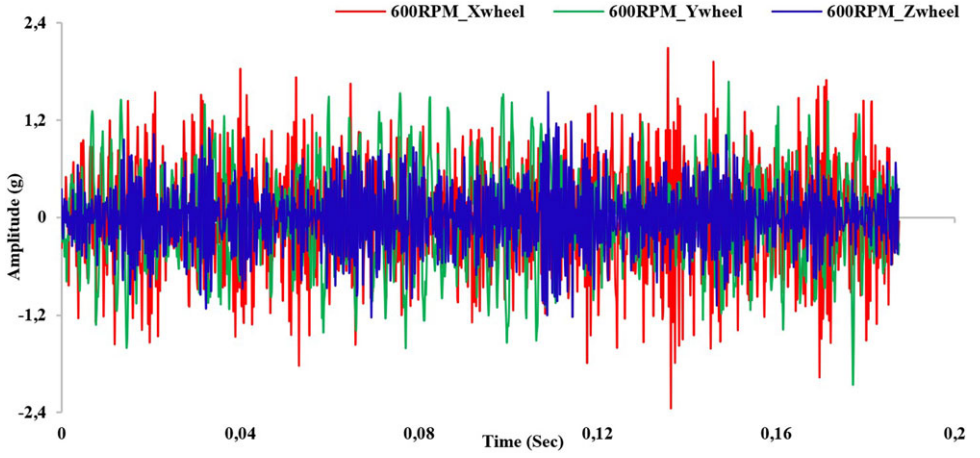

Figure 11. *Disturbance noise level vs. time for X, Y and Z wheels at 600 RPM.*

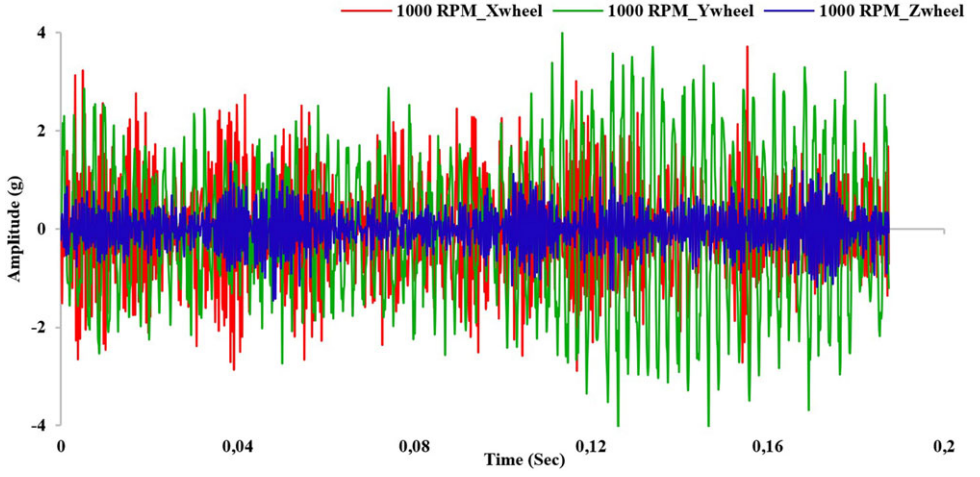

Figure 12. *Disturbance noise level vs. time for X, Y and Z wheels at 1,000 RPM.*

https://doi.org/10.1017/aer.2024.41 Published online by Cambridge University Press

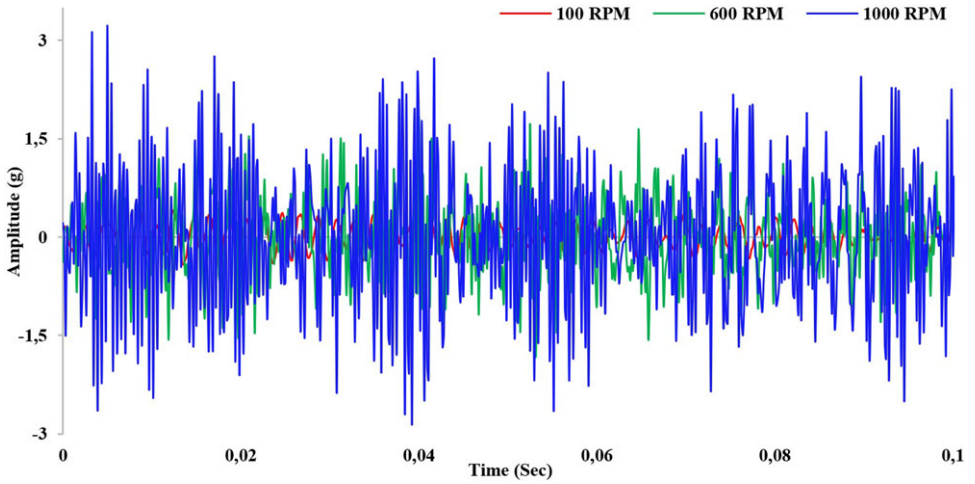

Figure 13. *Disturbance noise level vs. time for different RPM of X wheel.*

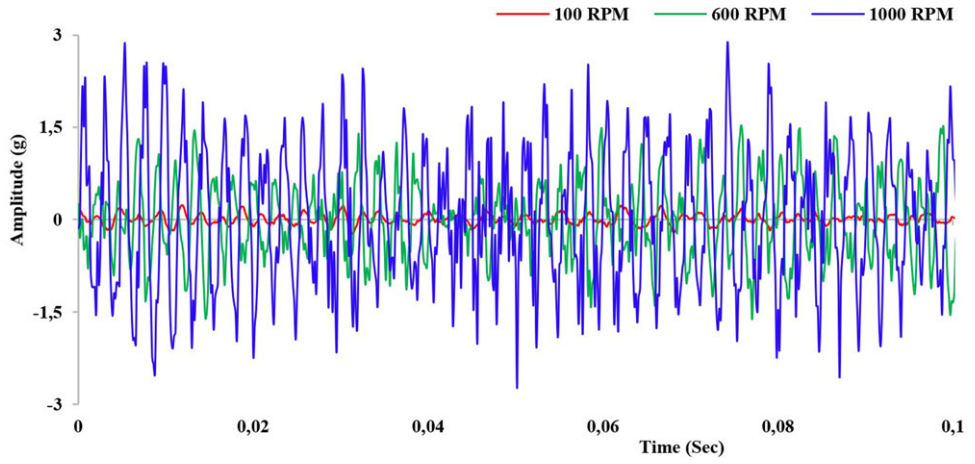

Figure 14. *Disturbance noise level vs. time for different RPM of Y wheel.*

spacecraft's attitude control system, plays a pivotal role in various aspects. These include monitoring the health of RWs and designing efficient attitude control systems [18].

3.2.2 Wheels rotation speed effect

In order to investigate the effect of wheel rotation on the level of disturbance noise, we had reported the results for three different rotations speed (100, 600 and 1,000) RPM. The rotational speeds were chosen to cover low, medium and high ranges, enabling the identification of their respective impacts on the produced disturbance noise amplitude and to better show the variation of noise level for different wheels speed. These speeds envelope the planned mission's wheel rotational speed profile, ranging between 300 and 800 RPM, as depicted in Fig. 3. The experimental data was extracted from the three wheels. For the clarity of the figures, we had taken only 0.1 sec test range.

The experimental results of the three wheels presenting the disturbance levels for different rotational speed were illustrated in Figs. 13–15. It was found that the disturbance levels are proportional to the rotational speed for the tree wheels test cases, as the modes of wheel structural will be excited by increasing

https://doi.org/10.1017/aer.2024.41 Published online by Cambridge University Press

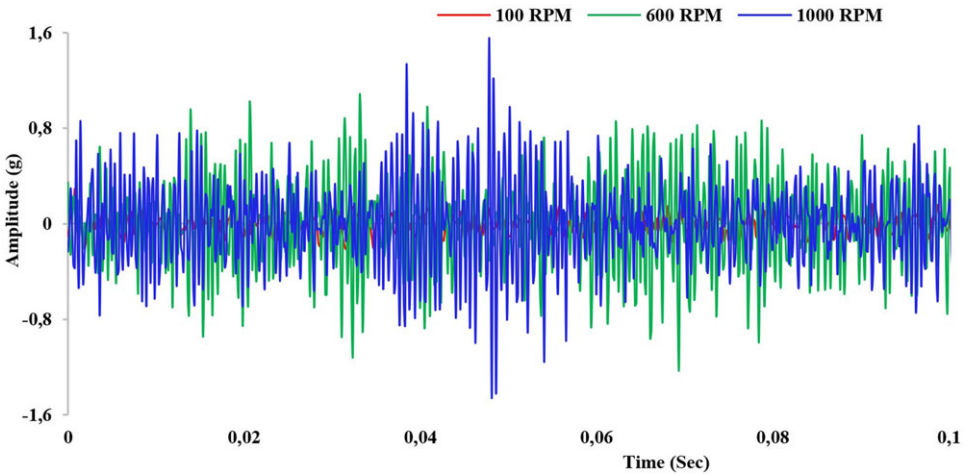

Figure 15. *Disturbance noise level vs. time for different RPM of Z wheel.*

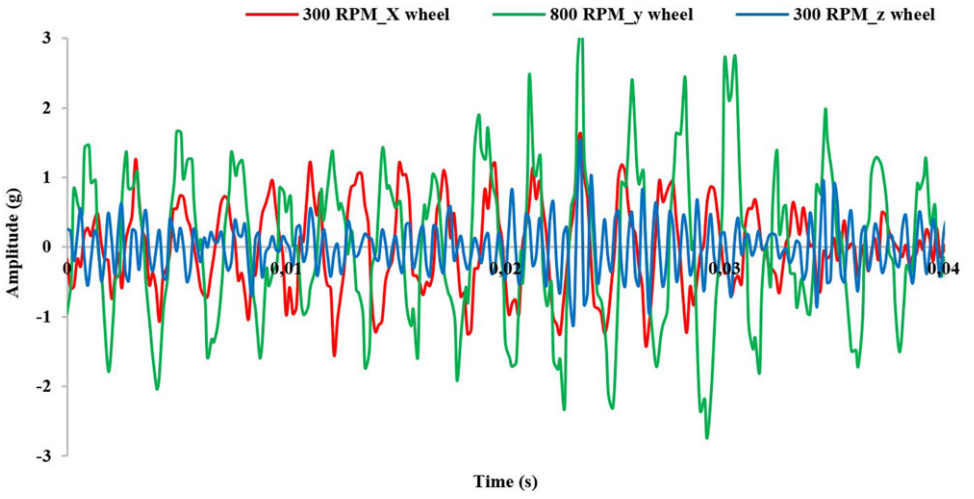

Figure 16. *Wheels noise for the worst-case scenario.*

speed [5, 9, 43, 44]. Hence, the wheels running at 1,000 RPM is dominant regarding disturbance level. In addition, the wheel towards X direction presents the highest value (3.2 g). Consequently, the optimisation of rotational speed allocated for the satellite stabilisation is a key factor to minimise noise level and, thus reduce microvibrations transferred to the payload. The ground test for disturbance noise quantification on flight spacecraft is an alternative methodology to measure microvibration levels for the success of the mission. Moreover, other solutions for disturbance reduction based on RWs with liquid lubricant in flight operation were used by Ref. [42], which generate low vibration levels. The finding can give an insight for balancing the need for precise attitude control with the potential drawbacks of high rotation speeds to ensuring the success of Earth observation satellite missions. Note that the Atitude and Orbit Control System (AOCS) wheel profile scenario created as worst case (see Fig. 2) with margins. Maximum wheel speeds during imaging operations will not reach 800 rpm. Hence, Alsat-1B Y wheel will be the main source of noise for the platform (800 rpm and 600 rpm) and X, Z wheel will be run at a max of 300 rpm (see Fig. 16). Hence, the jitter level for wheels speed gives an insight of the

https://doi.org/10.1017/aer.2024.41 Published online by Cambridge University Press

adopted attitude control profile for the mission considered as worst-case scenario to predict the risks of microvibrations.

4.0 Conclusion

Microvibrations resulting from reaction wheel noise significantly impact the precision of satellite system stabilisation, thus affecting image quality. Testing and measuring disturbance noise from RWAs are vital for effective satellite stabilisation management. Therefore, the measurement of disturbance noise level transferred to the satellite structure from spinning wheels assembled to proto-flight model provides a practical simulation close to on-orbit conditions. The conclusions drawn from this testing are:

- The test results demonstrate variations in disturbance noise levels among the same class wheels operating at identical speeds, highlighting the influence of manufacturing imperfections and anomalies on the generated noise levels. Consequently, quantifying noise disturbances for each individual balanced wheel remains imperative, particularly for missions with sensitive payloads susceptible to microvibration.
- The proportionality trend between wheel rotational speed and noise disturbance levels emphasises the importance of optimising mission rotational speed profiles to mitigate microvibration risks. Therefore, implementing an attitude control profile with lower rotation speeds of reaction wheels effectively reduces microvibration levels and minimises risks to payload performance. Consequently, ensuring optimal satellite operation with lower power consumption.

Consequently, the proposed test methodology effectively assesses disturbances transmitted to the satellite structure by reaction wheels in flight configuration. The gathered test data will be utilised for the development and calibration of numerical model, enabling us to accurately estimate the impact of microvibration levels on optical payloads housed within the satellite.

Acknowledgements. The authors wish to thank the Algerian space agency (ASAL) and Surrey Satellite Technology (SSTL) for their support to perform these tests on Alsat-1B and obtain the test results.

Competing interests. We confirm that the manuscript has been read and approved by all named authors and no conflict of interest exists. We wish to confirm that there are no known conflicts of interest associated with this publication and there has been no significant financial support for this work that could have influenced its outcome.

References

[1] Zhang Z., Yang L. and Pang S. Jitter environment analysis for micro-precision spacecraft. *Spacecr. Environ. Eng.*, 2009, **26**, (6), pp 528–534.
[2] Addari D. A semi-empirical approach for the modelling and analysis of microvibration sources on-board spacecraft. Chapter 2, PhD Thesis, University of Surrey, 2016.
[3] Cui Y., Feng Z. and Liu J. Micro-vibration influencing characteristic on image quality and solutions for high-resolution satellites. *Adv. Astronaut. Sci. Technol.*, 2019, **2**, 7–13.
[4] Rinard L.A., Chapman E.L. and Ringler S.C. Reaction wheel susplier survey. Aerospace Report No. ATR-2011(5389)-2, 2011.
[5] Dennehy C.J. A survey of reaction wheel disturbance modeling approaches for spacecraft line-of-sight jitter performance analysis. *European Space Mechanisms and Tribology Symposium*, 2019, Munich, Germany.
[6] Toyoshima M., Takashi J., Takahashi N., Toshihiko Y., Nakagawa K. and Katsuyoshi A. Transfer functions of microvibrational disturbances on a satellite. *Proceedings of the 2st International Communications Satellite Systems Conference and Exhibit*, Yokohama, Japan, 2003. doi: 10.2514/6.2003-2406
[7] Xia M., Qin C., Wang X. and Xu Z. Modeling and experimental study of dynamic characteristics of the moment wheel assembly based on structural coupling. *Mech. Syst. Signal Process.*, 2021, **146**, p 107007.
[8] Li L., Zhou M., Zhu Y., Dai Y. and Liang X. Satellite microvibration measurement based on distributed compressed sensing measurement. *Measurement*, 2022, **203**, p 112031.
[9] Nagabhushan V. and Fitz-Coy N.G. On-orbit jitter control in momentum actuators using a three-flywheel system. *Acta Astronaut.*, 2013, **95**, 61–81.

https://doi.org/10.1017/aer.2024.41 Published online by Cambridge University Press

[10] Dae-Kwan K. Micro-vibration model and parameter estimation method of a reaction wheel assembly. *J. Sound Vib.*, 2014, **333**, pp 4214–4231.
[11] Mankour A., Smahat A., Guy R., Wang R. and Khatir M. Experimental investigation of microvibrations induced by reaction wheels on earth observation satellite. *Adv. Space Res.*, 2021, **68**, (11), pp 4484–4495.
[12] Tkachev S., Mashtakov Y., Ivanov D., Roldugin D. and Ovchinnikov M. Effect of reaction wheel imbalances on attitude and stabilization accuracy. *Aerospace*, 2021, **8**, (9), p 252. doi: 10.3390/aerospace8090252
[13] Masterson R., Miller D. and Grogan R. Development and validation of reaction wheel disturbance models: empirical model. *J. Sound Vib.*, 2002, **249**, (3), pp 575–598.
[14] Liu K., Maghami P. and Blaurock C. Reaction wheel disturbance modeling, jitter analysis, and validation test for solar dynamics observatory. *AIAA Guidance, Navigation and Control Conference and Exhibit*, 18–21 August 2008, Honolulu, Hawaii, 2008. doi: 10.2514/6.2008-7232
[15] Taniwaki S., Kudo M., Sato M. and Ohkami Y. Analysis of retainer induced disturbances of reaction wheel. *Trans. Jpn. Soc. Mech. Eng. Ser. C*, 2005, **71**, (701), pp 21–28.
[16] Hatutori Y., Ohkami Y. and Taniwaki S. Experiment and analysis of reaction wheel disturbance with periodical torque applied. *Trans. Jpn. Soc. Mech. Eng. Ser. C*, 2004, **70**, (695), pp 1944–1950.
[17] Bialke B. Microvibration disturbance sources in reaction wheels and momentum wheels. *ESA SP Spacecr. Struct. Mater. Mech. Test.*, 1996, **386**, (2), pp 765–770.
[18] Taniwaki S. and Ohkami, Y. Experimental and numerical analysis of reaction wheel disturbance. *JSME Int. J. Ser. C*, 2003, **46**, (2), pp 519–526.
[19] Shengmin G. and Hao C. A comparative design of satellite attitude control system with reaction wheel. *Proceedings of First NASA/ESA Conference on Adaptive Hardware and Systems*, IEEE, Istanbul, Turkey, 2006, pp 359–362. doi: 10.1109/AHS.2006.2.
[20] Hodge C., Stabile A., Aglietti G. and Richardson G. The effect of assembly and static unbalance on reaction wheel assembly bearing harmonics, *CEAS Space J.*, 2020, **13**, pp 269–289.
[21] Luyang T. Design and dynamic optimization on integrated structure of satellite main bearing structure and optical cameraD. University of Chinese Academy of Sciences (Changchun Institute of Optics, Fine Mechanics and Physics, Chinese Academy of Sciences), 2017.
[22] Mankour A. Investigation on micro-vibration induced by reaction wheels. *J. Chin. Soc. Mech. Eng.*, 2020, **41**, (3), pp 325–335.
[23] Inamori T., Wang J., Saisutjarit P. and Nakasuka S. Jitter reduction of a reaction wheel by management of angular momentum using magnetic torquers in nano- and micro-satellites. *Adv. Space Res.*, 2013, **52**, pp 222–231.
[24] Lee D.O., Park G. and Han J.H. Hybrid isolation of micro vibrations induced by reaction wheels. *J. Sound and Vib.*, 2016, **363**, pp 1–17.
[25] Zhang Y., Guo Z., He H., Zhang J., Liu M. and Zhou Z. A novel vibration isolation system for reaction wheel on space telescopes. *Acta Astronaut.*, 2014, **102**, pp 1–13.
[26] Kong Y. and Huang H. Vibration isolation and dual-stage actuation pointing system for space precision payloads. *Acta Astronaut.*, 2018, **143**, pp 183–192.
[27] Luo Q., Li D. and Jiang, J. Analysis and optimization of microvibration isolation for multiple flywheel systems of spacecraft, *AIAA J.*, 2016, **54**, pp 1719–1731.
[28] Yun H., Liu L., Li Q. and Yang H. Investigation on two-stage vibration suppression and precision pointing for space optical payloads. *Aerosp. Sci. Technol.*, 2020, **96**, p 105543.
[29] Li L., Wang L., Yuan L., Zheng R., Wu Y., Sui J. and Zhong J. Micro-vibration suppression methods and key technologies for high-precision space optical instruments. *Acta Astronaut.*, 2021, **180**, pp 417–428.
[30] Kamesh D., Pandiyan R. and Ghosal A. Passive vibration isolation of reaction wheel disturbances using a low frequency flexible space platform. *J. Sound Vib.*, 2012, **331**, (6), pp 1310–1330. doi: 10.1016/j.jsv.2011.10.033
[31] Poncet D., Glynn S. and Heine F. Hosting the first EDRS payload. In *International Conference on Space Optics — ICSO, 2014*, edited by B. Cugny, Z. Sodnik, and N. Karafolas: SPIE, 2017. doi: 10.1117/12.2304091
[32] Weiyong Z. and Dongxu L. Experimental research on a vibration isolation platform for momentum wheel assembly. *J. Sound Vib.*, 2013, **332**, pp 1157–1171.
[33] Zhu L. Reaction spheres for attitude control of microsatellites. [Dissertation (TU Delft), Delft University of Technology], 2021. doi: 10.4233/uuid:9d0f7b28-dc4e-43b8-b838-84dc15b19b04
[34] UK-DMC-2 (United Kingdom-Disaster Monitoring Constellation-2). https://www.eoportal.org/satellite-missions/uk-dmc-2#uk-dmc-2-operations-and-performance
[35] Elwood A., Roland B., Carlino R., et al. State of the Art Small Spacecraft Technology. NASA Ames Research Center, Small Spacecraft Systems Virtual Institute. NASA/TP-2018-220027, 2018.
[36] Cheon D.I., Jang E.J. and Oh H.S. Satellite actuator balancing based on the disturbance measurement table data. *International Conference on Renewable Energies and Power Quality (ICREPQ'12) Santiago de Compostela (Spain)*, 28th to 30th March, 2012, Renewable Energy & Power Quality Journal (RE&PQJ), Spain, April 2012, pp 601–604.
[37] Narayan S.S., Nair P. and Ghosal A. Dynamic interaction of rotating momentum wheels with spacecraft elements. *J. Sound Vib.*, 2008, **315**, (4–5), pp 970–984.
[38] Longato M.M., Thomas H., Vladimir Y. and Guglielmo S.A. Microvibration simulation of reaction wheel ball bearings. *J. Sound Vib.*, 2023, **567**, p 117909. doi: 10.1016/j.jsv.2023.117909
[39] Fang T., Spoor P., Ghiaasiaan S. and Perrella M. Influence of minor geometric features on stirling pulse tube cryocooler performance. *IOP Conf. Ser.: Mater. Sci. Eng.*, 2017, **278**, (1), p 012140. doi: 10.1088/1757-899X/278/1/012140

[40] Rafsanjani A., Abbasion S., Farshidianfar A. and Moeenfard H. Nonlinear dynamic modeling of surface defects in rolling element bearing systems. *J. Sound Vib.*, 2009, **319**, (3–5), pp 1150–1174.
[41] Butterfield A.J. and Woodard S.E. Measured spacecraft instrument and structural interactions. *J. Spacecr. Rockets*, 1996, **33**, (4), pp 556–562.
[42] Grau S., Kapitola S., Weiss S. and Noack D. Control of an over-actuated spacecraft using a combination of a fluid actuator and reaction wheels. *Acta Astronaut.*, 2021, **178**, pp 870–880.
[43] Wang H., Chen L., Jin Z., Crassidis J.L. Adaptive momentum distribution jitter control for microsatellite. *J. Guid. Contr. Dyn.*, 2018, **42**, (3), pp 632–642. doi: 10.2514/1.G003909
[44] Li L., Tan L., Kong L., Wang D. and Yang H. The influence of flywheel microvibration on space camera and vibration suppression. *Mech. Syst. Signal Process*, 2018, **100**, pp 360–370. doi: 10.1016/j.ymssp.2017.07.029

Cite this article: Mankour A., Smahat A., Bensikaddour E.H. and Roubache R. Experimental analysis of noise disturbances generated by reaction wheel. *The Aeronautical Journal*, https://doi.org/10.1017/aer.2024.41